Low-Pressure, Metastable Growth of Diamond and "Diamondlike" Phases

John C. Angus and Cliff C. Hayman

Diamond may be grown at low pressures where it is the metastable form of carbon. Recent advances in a wide variety of plasma and electrical discharge methods have led to dramatic increases in growth rates. All of these methods have certain aspects in common, namely, the presence of atomic hydrogen and the production of energetic carbon-containing fragments under conditions that support high mobilities on the diamond surface. Some understanding of the processes taking place during nucleation and growth of diamond has been achieved, but detailed molecular mechanisms are not yet known. Related research has led to the discovery of a new class of materials, the "diamondlike" phases. Vapor-grown diamond and diamondlike materials may have eventual applications in abrasives, tool coatings, bearing surfaces, electronics, optics, tribological surfaces, and corrosion protection.

Of all crystalline solids, diamond holds a special position. Its name is derived from the Greek *adamas*, meaning "unconquerable, invincible." Synthesis of diamond has attracted attention ever since it was established in 1797 that diamond is a crystalline form of carbon. Initially, high pressures were used simply because diamond is the densest carbon phase. As understanding of chemical thermodynamics developed throughout the 19th and 20th centuries, the pressure-temperature range of diamond stability was explored. These efforts culminated in the announcement in 1955 of a process for diamond synthesis with a molten transition metal solvent-catalyst at pressures where diamond is the thermodynamically stable phase (*1*). Synthetic diamond made by high-pressure processes is now a commonplace item of commerce.

Less well known has been a parallel effort directed toward the growth of diamond at low pressures, where it is metastable. Although diamond was successfully produced, low-pressure synthesis was plagued by extremely low growth rates, no greater than 0.1 μm hour^{-1}. Recent developments have led to much higher growth rates, creating enormous interest in the field. Polycrystalline diamond films can now be produced on a variety of substrates at growth rates of tens of micrometers per hour. In addition, the discovery of an entirely new class of solids known as "diamondlike" carbons and hydrocarbons has arisen out of this work. In this article, we review the characteristics and synthesis of crystalline diamond grown at low pressure, the diamondlike hydrocarbons (a–C:H), and the diamondlike carbons (a–C) (Fig. 1).

Structure and Properties of Diamond

The diamond-cubic lattice consists of two interpenetrating face-centered cubic lattices, displaced by one quarter of the cube diagonal. Each carbon atom is tetrahedrally coordinated, making strong, directed σ bonds to its neighbors using hybrid sp^3 atomic orbitals. The lattice can also be visualized as planes of six-membered saturated carbon rings stacked in an ABC ABC ABC sequence along <111> directions. Each ring is in the "chair" conformation and all C–C bonds are staggered.

A lattice with hexagonal symmetry, lonsdaleite, can be construct-

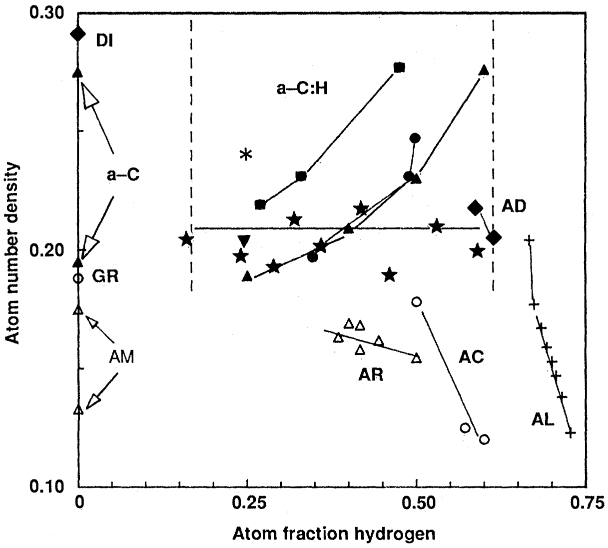

Fig. 1. Atom number density versus atom fraction hydrogen expressed in gram-atoms per cubic centimeter, which is the total number of atoms per cubic centimeter divided by Avogadro's number. This type of plot provides a convenient way for categorizing different classes of hydrocarbons and carbons (*2*). Similar compounds, for example the *n*-alkanes (AL), fall in tight groupings on the diagram. Diamond, DI, is at the upper left-hand corner. The adamantanes, AD, which are 10 and 14 carbon atom molecular diamonds, are at the lower right of the diamondlike hydrocarbon (a–C:H) grouping. The diamondlike hydrocarbons (filled symbols) range from approximately 0.20 to 0.60 atom fraction hydrogen and have number densities greater than 0.19 gram-atom per cubic centimeter. The vertical dashed lines show the theoretical composition range predicted by Eq. 6 for fully constrained, random hydrocarbon networks. The atom number density of a–C:H increases with hydrogen content in contrast to the behavior of conventional hydrocarbons. This increase is caused by the increase in average coordination number of carbon from 3 to 4 as the amount of hydrogen is increased. The diamondlike carbons (a–C) appear to be a different class of material with little or no hydrogen and with atom number densities from approximately 0.19 to 0.28 gram-atom per cubic centimeter. These densities indicate significant sp^3, tetrahedral, bonding. The amorphous carbons (AM) are dominated by sp^2, trigonal, bonding and can be formed by laser or electron-beam evaporation. Other symbols are: AC, oligomers of acetylene; AD, adamantanes; AR, polynuclear aromatics; and GR, graphite. References for a–C:H: ●, (*2*); ▲ (*102*); ▼ (*103*); ★ (*104*); * (*105*); ■ (*106*).

The authors are in the Department of Chemical Engineering, Case Western Reserve University, Cleveland, OH 44106.

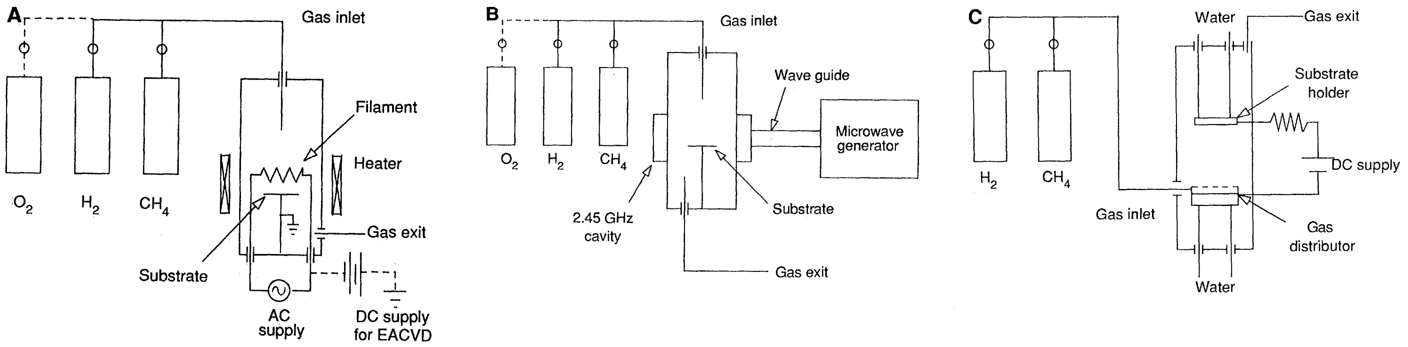

Fig. 2. Schematic drawings of several techniques for diamond synthesis at low pressures; (**A**) hot filament–assisted chemical vapor deposition (HFCVD), in which a hot filament is used to generate atomic hydrogen near the substrate. Also shown in dashed lines are the changes required to add an oxygen-containing gas and to operate the system in the electron-assisted mode (EACVD); (**B**) a plasma-assisted deposition using a microwave cavity; (**C**) a DC discharge method (*41, 46*).

ed with the same tetrahedral nearest neighbor configuration. In lonsdaleite, however, the planes of chairs are stacked in an AB AB AB sequence. The C–C bonds normal to these planes are eclipsed. In simple organic molecules, the eclipsed conformation is usually less stable than the staggered because steric interactions are greater. This may be the reason that the dominant polytype for both natural and synthetic diamonds is the cubic structure.

Thermodynamically, diamond is slightly unstable with respect to crystalline graphite. At 298 K and 1 atm the free energy difference is 0.03 eV per atom, only slightly greater than kT. In the absence of a catalyst, however, such as a liquid metal that can dissolve carbon, there is a large activation energy barrier between the two phases.

The great interest in diamond stems from its extreme properties. Diamond has the highest atom number density of any material at terrestrial pressures (*2*). [A possible exception is the superdense carbon phase reported by Matyusenko *et al.* (*3*).] As a result of its high atom-number density and the strong covalent bonding, diamond has the highest hardness and elastic modulus of any material and is the least compressible substance known (*4*). The thermal conductivity of diamond at 300 K is higher than that of any other material and its thermal expansion coefficient at 300 K is 0.8×10^{-6}, lower than that of Invar. Diamond is a very wide band gap semiconductor ($E_g = 5.5$ eV), has a high breakdown voltage (10^7 V cm^{-1}), and its saturation velocity of 2.7×10^7 cm s^{-1} is significantly greater than that of silicon, gallium arsenide, or indium phosphide (*5, 6*).

Applications of Vapor-Grown Diamond

Applications of vapor-grown diamond actually in the marketplace or close to commercialization are few. They include a high-range audio-speaker diaphragm and a coating on cutting tools (*7*). The largest commercial impact within the next few years may be the growth of different grades of abrasive grit by vapor methods.

There is great interest in using single-crystal diamond for heat sinks and as an active semiconductor element. Potential electronic applications of diamond include high temperature devices (*8*), millimeter-wave traveling wave amplifiers (*9*), backward wave oscillators (*10*), and picosecond high-voltage electro-optic switches (*11*). Excimer laser patterning of natural diamond and diamondlike carbon for microelectronic devices has been demonstrated (*12*). Some potential applications may require only polycrystalline films, for example, laser and x-ray windows, lenses, bearing surfaces, and tribological coatings.

Many applications of vapor-grown diamond require significant advances to become realized. A method of heteroepitaxial growth is required for most electronic applications. Even in the simpler case of homoepitaxy, vapor-grown diamond has been shown to be highly defective, with microcracking along (111) planes (*13*). Diamond laser windows, x-ray windows, lens coatings, and optical structures should eventually be possible, but current diamond films are too rough and imperfect for these uses.

History of Metastable Diamond Growth

Metastable phases can form from precursors with high chemical potential if the activation barriers to more stable phases are sufficiently high. As the precursors fall in energy, they can be trapped in a metastable configuration. Formation of a metastable phase depends on selecting conditions where rates of competing processes to undesired products are low (*14*). In the case of diamond, achieving the appropriate conditions has taken decades of research (*15*). The processes competing with diamond growth are spontaneous graphitization of the diamond surface and nucleation and growth of graphitic deposits.

W. G. Eversole at the Union Carbide Corporation was the first to grow diamond successfully at low pressures. His work was initiated in 1949, and he achieved growth on diamond seed crystals in the period 26 November 1952 to 7 January 1953 (*16*). Conclusive proof and repetition of the experiments took place from 17 February 1953 to 15 October 1953 (*16*). This predates the successful diamond synthesis at high pressure by workers at the General Electric Company, which was accomplished in December 1954 (*17*) and announced publicly in 1955 (*1*). It is essentially contemporaneous with the date of 15 February 1953 indicated by Liander for the first synthesis of diamond at Allemanna Svenska Elektriska Aktiebolaget (ASEA) in Sweden (*18*). Eversole may have been the first to create new diamond by any method. Eversole grew new diamond on preexisting diamond nuclei; the General Electric and ASEA syntheses started with nondiamond carbons.

B. Deryagin in the Soviet Union, who started work on low-pressure diamond synthesis in 1956 (*19*), has had the longest sustained research effort on metastable diamond growth of any worker. Deryagin's group has taken many approaches, starting with growth of diamond whiskers by a metal-catalyzed vapor-liquid-solid (VLS) process. His group subsequently investigated epitaxial growth from hydrocarbons and hydrocarbon-hydrogen mixtures, and different forms of vapor transport reactions. They also performed theoretical investigations of the relative nucleation rates of diamond and graphite (*20*); for an excellent review see (*21*).

Angus and co-workers at Case Western Reserve University

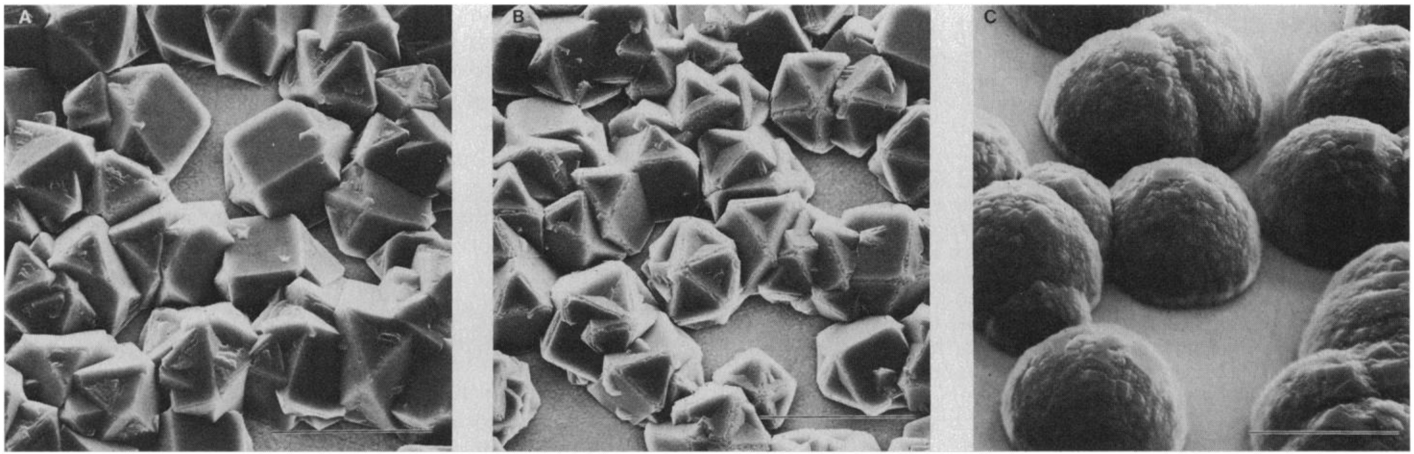

Fig. 3. Diamond crystals grown by chemical vapor deposition using a combined microwave and hot filament method. The source gas was 1.5% methane in hydrogen at 10 torr. Cube and octahedral faces are evident in (**A**); note the twinned crystals with pseudo-fivefold symmetry in (**B**); (**C**) ball-like diamonds grown at high supersaturations; the scale is 12 μm in (A) and (B) and 15 μm in (C). [Microphotographs are courtesy of T. Anthony of the General Electric Company, Schenectady, New York]

concentrated primarily on chemical vapor deposition of diamond on diamond seed crystals from hydrocarbons and hydrocarbon-hydrogen mixtures (*22*). They grew *p*-type semiconducting diamond from CH_4-B_2H_6 gas mixtures and studied the rates of diamond and graphite growth in CH_4-H_2 gas mixtures and ethylene. They were the first to report on the preferential etching of graphite compared to diamond by atomic hydrogen and noted that boron had an unusual catalytic effect on metastable diamond growth.

The role of hydrogen in permitting metastable diamond growth was a constant thread throughout the early work. The low energy electron diffraction (LEED) study of Lander and Morrison (*23*) is the most significant. They showed that a (111) diamond surface gave an unreconstructed (1 by 1) LEED pattern. The unsatisfied dangling bonds normal to the surface are terminated with hydrogen atoms, which maintain the integrity of the lattice to the outermost surface layer of atoms. When hydrogen is absent, the surface reconstructs into more complex structures. Lander and Morrison also showed that carbon atoms are very mobile on the diamond surface at temperatures above 1200 K and pointed out that these conditions could lead to epitaxial growth of diamond.

Several workers showed that the presence of hydrogen enhanced yields of diamond (*24*). Chauhan *et al.* (*25*) and Fedoseev *et al.* (*26*) showed that addition of hydrogen to the hydrocarbon gas phase suppressed the growth rate of graphite more than it suppressed the growth rate of diamond, resulting in higher diamond yields. Eventually, however, graphitic carbons nucleated on the surface and suppressed further diamond growth. It was then necessary to remove the graphitic deposits preferentially, with atomic hydrogen (*27*) or oxygen (*28*), and to repeat the sequence.

By the mid-1970s diamond growth at low pressures had been achieved by several groups. The beneficial role of hydrogen was known and understood to some extent and transient growth rates of 0.1 $\mu m\ hour^{-1}$ (*25*) had been achieved. However, net growth rates were too slow to be of practical commercial importance. Nevertheless, these results provided the experimental foundation for much of the work that followed.

Modern Era of Metastable Diamond Growth

The most significant initiative in recent years has been a large program in metastable diamond growth started in 1974 at the National Institute for Research in Inorganic Materials in Japan. Principal workers included N. Setaka, S. Matsumoto, M. Kamo, and Y. Sato among others (*29*). In a series of remarkable papers starting in 1982, they described techniques for synthesizing diamond at rates of several micrometers per hour from microwave or DC discharges or from gases decomposed by a hot filament (*30*). These processes produced individual faceted crystals without the use of a diamond seed crystal. Deryagin had reported high rate growth of diamond earlier (*31*); however, he did not reveal his method. All of the methods are based on the generation of atomic hydrogen near the surface while growth is proceeding.

In the mid-1970s efforts were made to grow diamond by various ion beam processes. In 1973 Aisenberg and Chabot (*32*) deposited hard carbon films using a beam of carbon ions. Although these films had many of the properties of diamond, they were called diamondlike carbon because definitive diffraction identification was not possible [see also (*33*)]. In 1976 Spencer *et al.* formed finely divided polycrystalline diamond using a beam of carbon ions with energies between 50 and 100 eV (*34*) and, subsequently, Freeman grew diamond by ion implantation (*35*).

These seminal studies have led to a wide range of research, not only on diamond, but also on diamondlike carbon and hydrocarbons. The most successful growth method has been in the deposition of diamond from hydrocarbon-hydrogen gas mixtures, However, there has been investigation of other methods for metastable growth as well, for example, Patel and Cherian grew diamond from a molten salt in the presence of Ni (*36*).

Diamond Synthesis by Chemical Vapor Deposition (CVD)

Techniques for growing diamond metastably may be conveniently divided into three categories: hot filament chemical vapor deposition (HFCVD); high frequency plasma-assisted chemical vapor deposition (PACVD); and DC plasma discharge. Hybrid techniques, for example, hot filaments immersed in a plasma discharge, have also been used.

In HFCVD (Fig. 2A) (*37*), a tungsten filament or foil at 2000 to 2800 K is used to dissociate gas mixtures containing from 0.2 to 2.0% CH_4 in H_2, typically at about 6000 Pa but also up to atmospheric pressure. The dissociation products at these tempera-

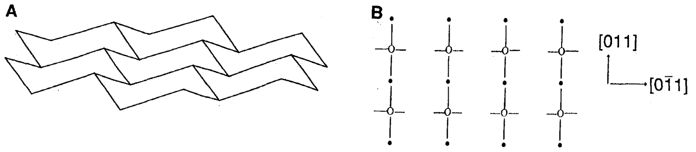

Fig. 4. Unreconstructed diamond surfaces and nucleation sites. (**A**) A section of an unreconstructed (111) surface layer; the lower atoms are bonded to atoms in the crystal. The upper atoms have one unpaired electron and form a vacant surface site. Hydrogen atoms can occupy these sites. (**B**) A top view of the unreconstructed (100) surface. Atoms marked with an "O" are in the top layer and are bonded twice to the rest of the lattice; atoms marked "●" are in the second layer and are bonded four times to the lattice. Vacant two-bonded surface sites lie between the "O" atoms. Addition of single carbon atoms to these sites leads to extension of the diamond-cubic lattice.

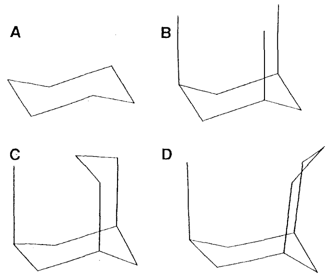

Fig. 5. An element of the (111) surface (**A**), an element of the surface with three carbon atoms (or methyl groups) attached (**B**), and the start of cubic (**C**) and hexagonal (**D**) nuclei on the surface element. Cubic and hexagonal nuclei differ only in next-nearest neighbor interactions. In a cubic nucleus the C–C bonds to the surface are in the staggered conformation; therefore, steric interactions with the surface plane are minimized. All six-membered rings are chairs. The hexagonal nucleus is formed when the C–C bonds are eclipsed, that is, the middle atom of the three-atom bridge is directly above an atom in the surface plane. This leads to a six-membered ring with the boat conformation. Extension of either nucleus across the (111) plane can be accomplished by addition of single-carbon and two-carbon atom species. Layer growth from a cubic nucleus in this manner will lead to an extension of the diamond-cubic lattice. Extension of a hexagonal nucleus across the (111) surface of a diamond-cubic lattice will lead to a twin plane.

tures consist mainly of radicals, for example, CH_2, C_2H, and CH, acetylene, and atomic hydrogen, as well as unreacted CH_4 and H_2 (*38*). Filaments of W, Ta, Mo, and Re have been used to produce diamond (*39*), but Pt filaments have given only graphitic deposits (*39, 40*). Graphite deposition may be related to the enhanced recombination rate of atomic hydrogen or other radicals on Pt or simply a result of the lower filament temperature. The filament is typically placed within 1 cm of the substrate surface to minimize thermalization and radical recombination. However, radiation heating can produce excessive substrate temperatures leading to nonuniformity and even graphitic deposits (*41*).

One approach to the problem of excessive radiation heating has been to withdraw the filament slightly and bias it negatively to provide an electron current to the substrate (Fig. 2A). Electron impact enhances the reactivity of graphite to atomic hydrogen by excitation of π electrons (*42*) and also enhances the fragmentation of hydrocarbons at or near the substrate surface. Electron-assisted, chemical vapor deposition (EACVD) can increase the initial nucleation rate compared to HFCVD, permitting the deposition of diamond at lower substrate temperatures. Diamond growth at an average substrate temperature of 823 K has been reported (*43*), but the true surface temperature may have been higher. In some cases the effect of electron bombardment may not have been separated from the influence of the DC plasma arc that also can form under EACVD conditions.

In PACVD (*44, 45*), power at 2.45 GHz is coupled to a plasma in a small-diameter tube within a wave guide or cavity (Fig. 2B). Diamond is deposited on an electrically floating substrate at about 60-Pa pressure under gas phase compositions similar to those of the hot-filament process. Substrate temperature is determined by the power density and the placement of the substrate. Microwave and RF (radio frequency) methods in which the substrate is removed from the plasma have been reported (*46*). Diamonds have also been grown in microwave discharges in a magnetic field, under conditions where electron cyclotron resonance is considerably modified by collisions. These "magneto-microwave" plasmas can have significantly higher densities and electron energies than isotropic plasmas and can be used to deposit diamond over large areas (*47*).

A stabilized, DC plasma arc (Fig. 2C) has produced growth rates of 20 μm hour^{-1} at the anode (*41*). Only graphitic deposits formed on the cathode. DC glow discharges (*48*) and DC plasma jet (*49*) methods for producing diamond have also been used. The DC plasma jet has been reported to produce diamond at high linear growth rates, up to 80 μm hour^{-1} (*49*). Diamond has also been produced in transient experiments, for example, by irradiation of C_2H_2 in H_2 (*50*) with focused ArF excimer laser pulses at 193 nm.

Common Factors and Differences in the Deposition Processes

A striking observation is the large number of methods that have been used to synthesize diamond. In the "thermal" methods such as hot filament, thermal plasmas, and DC plasma jet, the temperatures of the neutrals and the electrons are roughly equal and much greater than the substrate temperature. In microwave plasmas and DC glow discharges, however, the electron temperature (10,000 to 20,000 K) is typically much greater than the neutral and substrate temperatures (about 1000 K). Yet both thermal and nonthermal methods produce diamond, although the highest rates have been achieved with the thermal methods.

Atomic hydrogen is used in all of the processes. Apparently, it prevents surface reconstruction, suppresses the formation of unsaturated carbon nuclei, and etches any graphitic nuclei that may form.

Dissociation of the carbon-containing source gases is common to all of the processes. However, significant ionization does not appear to be critical because there is little ionization in the hot filament method. The population of excited state fragments is higher in a thermal plasma than in a glow discharge. However, because both the extent of dissociation and the gas phase chemistry are different, the role of particular excited state species is difficult to assess.

Substrate temperatures must be high enough to impart mobility of adsorbed surface species (1100 to 1250 K). Impingement of ions and neutrals, particularly H$^+$, can apparently produce locally equivalent surface conditions at much lower bulk substrate temperatures. However, the film produced is only partially crystalline (*51*).

All of the reported methods have a lower pressure limit. Below about 50 Pa only amorphous and graphitic carbon are deposited.

Properties of Diamonds Grown by CVD

Identification of vapor-grown diamond by diffraction and Raman spectroscopy is definitive and has been accomplished by many workers. Vapor-grown crystals show the characteristic hardness and thermal conductivity of diamond (*52*).

Diamonds grown from vapor (Fig. 3) are commonly bounded by octahedral {111} or cubic {100} planes or combinations of the two. At low temperature and supersaturation, crystals with {111} faces are observed and at high temperature and supersaturation {100} cube faces are dominant (*13, 53*).

Some vapor-grown diamonds have a slightly smaller lattice constant than natural or high-pressure synthetic diamonds (*13, 53*). Differences in the number and type of defects and slightly different impurity levels are also common. For example, diamonds grown by vapor deposition from hydrocarbons contain more hydrogen than natural diamonds or high-pressure synthetics.

Commonly, the sharp Raman line at 1332 cm^{-1} is broadened slightly in vapor-grown diamonds. In some diamonds, high fluorescence background and a broad Raman peak at approximately 1500 cm^{-1} have been observed (*48*).

Molecular Processes During Low-Pressure Diamond Growth

In the presence of atomic hydrogen the principal surfaces of diamond are likely to be saturated with hydrogen. Because the H–H bond energy is greater than the C–H bond energy, atomic hydrogen will both add to vacant surface sites, S·, and abstract hydrogen from filled sites, S–H

$$S\cdot + H\cdot \rightarrow S\text{–}H \qquad (1)$$

$$S\text{–}H + H\cdot \rightarrow S\cdot + H_2 \qquad (2)$$

Reactions 1 and 2 are exothermic. The required energy is supplied by the energy added to dissociate H_2 ($H_2 \rightarrow 2H\cdot$). Because of the dynamic interaction between atomic hydrogen and the surface, there will be a steady-state concentration of free surface sites, S·, which can undergo reactions with carbon-containing species, R, for example,

$$S\cdot + R\cdot \rightarrow S\text{–}R \qquad (3)$$

There has been much speculation about the nature of the growth sites and whether the intermediate for diamond growth is a single-carbon-atom species, for example, involving CH_3 radicals and CH_3^+ ions (*54*), or a two-carbon-atom species, for example, acetylene (*55*). Another intriguing possibility is the direct insertion of methylene radicals, CH_2, into the C–H bonds (*56*) on the hydrogen-saturated surface.

Methyl radicals are probably major species in nonthermal methods, at least at moderate power densities (*57*). Acetylene, CH_2, CH, and multicarbon fragments are more commonly the products of thermal dissociation (*38*). In the thermal methods, gradients in gas temperature and energy between the excitation source and substrate are large. Consequently CH_3 concentrations may be considerable at the film surface in these methods as well. The morphology of the crystals obtained in the microwave process depends only on the overall C/H in the plasma; this observation indicates that the intermediate diamond-forming species is a common decomposition product of the original source gas (*58*).

Experimental evidence in support of any growth mechanism is limited, but several workers have interpreted their results as favoring growth by the addition of single-carbon species. Kowato and Kondo (*37*) showed that oxygen reduced the concentration of acetylene and gave high quality diamond at high rates in the hot filament process. Sokolowski (*59*) has suggested that negative carbon ions are a diamond-forming intermediate. Mitsuda *et al.* proposed that a low C_2/H is a necessary condition for diamond formation from a microwave plasma (*60*). Chauhan *et al.* showed that the growth rate on diamond powders by thermal CVD was first order in methane partial pressure and one-half order in ethylene partial pressure (*25*). This result is strong evidence that one step in these experiments involved a single-carbon-atom species but does not preclude the easy addition of acetylenic species in later steps.

Plasma chemistry can affect the deposit in other ways. For example, at low pressures the dissociation of H_2 ($H_2 \rightarrow 2H$) increases, and the population of excited hydrogen, H^* [principally H(2*p*,2*s*)], increases as well (*61*). The level of ionization increases because a major ionization channel is through excited states (*62*). Consequently, the ratio of ion to neutral fluxes at the substrate increases. In DC plasmas ion bombardment at the cathode is enhanced. Highly exothermic reactions at the substrate may contribute to graphitization. Excited-state hydrogen may contribute to dissociation through de-excitation processes of the type:

$$H^*(2s) + CH_x \rightarrow CH_{x-1} + 2H(1s) \qquad (4)$$

The cross sections for the de-excitation reactions have been estimated to be as large as $\approx 10^{-15}$ cm^2 for $x = 1$ (*63*). Dissociative de-excitation and ion recombination are highly exothermic processes that may promote graphitization. This speculation is supported by a comparison of HFCVD and microwave methods, which represent the extremes in percent ionization. In HFCVD, in which there is little ionization, diamond particles are produced at pressures as low as 66.5 Pa, whereas at 532 Pa the magnetic microwave method gives graphitic carbon and some diamond (*47*).

Surface transport plays an important role in vapor growth of diamond. For example, during growth by a microwave process individual diamond particles undergo surface restructuring that yields large, well-defined crystal faces (*64*). The linear growth rate of an isolated diamond crystal on a substrate decreases as it grows larger, indicating that growth does not occur by direct attachment of vapor-phase species to the crystal surface (*39*). Apparently, growth is fed by surface diffusion from a zone on the substrate surrounding the perimeter of the crystal. If this zone were of constant width, its area would be proportional only to the linear dimensions of the crystal. Also, order of magnitude differences of rate have been observed on different substrates: growth rates are lowest on oxides, intermediate on metals and graphite, and the greatest on boron (*39*).

Influence of Surface Structure on Mechanism

Random insertion or addition to sites on a hydrogenated diamond surface will lead to an amorphous or polymeric deposit. The atomic structure of the surface must be directing adatoms to specific sites. Furthermore, growth mechanisms on the principal planes of diamond-cubic solids should differ because of the different types of vacant surface sites on the planes (*65*). These effects should be particularly strong on diamond because of its strong, directed covalent bonding (*66*).

An unreconstructed, smooth {111} diamond surface is composed of puckered hexagons (Fig. 4A). An unreconstructed {100} surface contains zigzag chains of atoms in the <011> and $<01\bar{1}>$ directions (Fig. 4B).

On {100} planes attachment of single-carbon-atom species, such as C, CH, or CH_2, is energetically favored because they can make two bonds with the surface. Furthermore, addition of carbon atoms to these two-bonded sites automatically extends the diamond-cubic lattice. On the other hand, the smallest, relatively strain-free nuclei on a {111} surface are a three-membered bridge and a four-membered nucleus (*67*). On smooth {110} surfaces, two-carbon-atom species form a strain-free bridge that can propagate along the $<1\bar{1}0>$ chain by single-carbon-atom addition.

These arguments indicate that the rates of addition of single-carbon-atom species to the principal surfaces are in the order {100} > {110} > {111}. The rapid addition of single carbon atoms to {100} planes will lead to faceted crystals with {111} faces. Rapid addition of atoms to {111} planes will lead to faceted crystals bounded by {100} cube faces.

This simple description is consistent with many observations. For example, growth on {100} planes is rapid at low supersaturations,

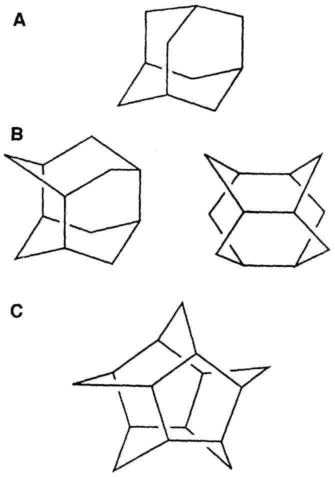

Fig. 6. Possible diamond nuclei proposed by Matsumoto and Matsui (*72*). The nuclei are fully saturated with hydrogen atoms that are not shown. (**A**) The adamantane molecule, which may be thought of as a ten-carbon molecular diamond. It is an untwinned diamond nucleus. All of the six-membered rings in adamantane are chairs, and all carbon-carbon bonds are staggered. (**B**) Tetracyclododecane, which contains a twin plane separating the two six-membered chairs. The three C–C connecting the two chairs are eclipsed. Tetracyclododecane is the molecular analog of lonsdaleite, the so-called "hexagonal" diamond. (**C**) Hexacyclopentadecane, which contains five twin planes. It may be the precursor of the twinned crystals with fivefold symmetry shown in Fig. 3B. DeVries (*15*) has shown a model of a large, multiply twinned diamond nucleus with pseudo-fivefold symmetry based on the hexacyclopentadecane nucleus.

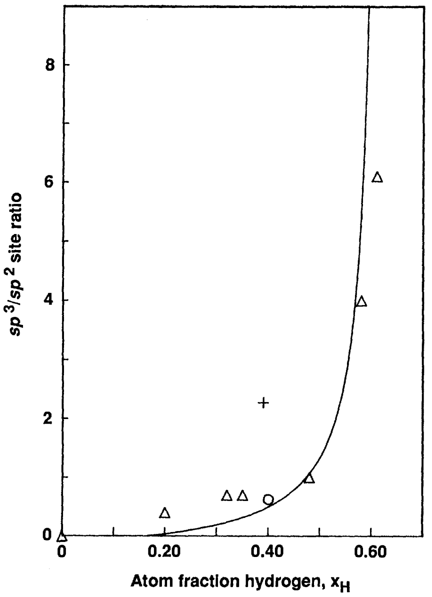

Fig. 7. The ratio of sp^3 to sp^2 sites in a–C:H; The points labeled △ are from (*104*), the point labeled ○ from (*87*) and the point labeled + from (*88*). The first two were obtained from NMR measurements, the last one from analysis of the infrared spectrum. The line is the theoretical expression (Eq. 6) obtained by Angus and Jansen (*83*) for a fully constrained, random hydrocarbon network.

and growth on {111} planes becomes rapid at high supersaturations where the probability of forming multicarbon nuclei is greater. Also, Fujimori (*68*) has reported that in diamond-on-diamond epitaxy, better crystallinity was achieved on {100} surfaces than on {111} surfaces.

Mechanisms of Diamond Nucleation

The initial nucleation mechanism of a diamond crystallite is distinct from the mechanism for the extension of a preexisting diamond lattice. Diamond nuclei form on many diverse substrates, but the atomic arrangement of the nucleation sites is unknown. Kawarada *et al.* have studied the silicon-diamond interface using high-voltage electron microscopy (*69*). They showed that a diamond crystal grew from a single nucleation site but did not determine the nature of the site. Nucleation rate is enhanced both by electron bombardment (*52*) and by scratching the substrate surface before growth (*60*). Some investigators have indicated that nucleation may occur on residual diamond particles or on other fragments (*70*); however, there is also evidence that, at least in some cases, diamond crystals actually nucleate in the vapor phase (*71*). The diamond crystals obtained by chemical vapor deposition commonly contain twins and multiple twins (Fig. 3B).

Matsumoto and Matsui (*72*) have proposed that several hydrocarbon cage compounds are possible embryos for vapor-grown diamond. Three of these are adamantane, tetracyclopentadecane, and hexacyclopentadecane (Fig. 6). Analogous nuclei, perhaps clusters with Si or various metals, may be more thermally stable at the growth temperatures and consequently even more likely candidates for diamond embryos. Metal-containing embryos would also explain the observed sensitivity of nucleation rates to impurity levels.

Diamondlike Hydrocarbon Phases

Diamondlike hydrocarbon phases (a–C:H) were apparently first noticed by Schmellenmeier in 1953 (*73*); however, their unusual structure and properties have been well understood only recently. The diamondlike hydrocarbons provide the limiting values of atom number density and cross-linking that are possible in a hydrocarbon structure (Fig. 1).

Because these diamondlike materials are hydrocarbons, their composition and properties can be varied. They can be made to be harder than silicon carbide and can be thought of as hydrocarbon ceramics. Diamondlike antireflective coatings with precisely controlled refractive index and thickness have been deposited on germanium infrared optics (*74*). Because of the extreme chemical resistance and nanometer-scale smoothness of a–C:H films, they may have applications as protective coatings for both magnetic and optical disks. The high differential etch selectivity (*75*) and clean laser ablation in reactive gases make a–C:H useful for advanced projection photolithography and perhaps for direct-write microelectronics (*12*).

Certain properties of the hard a–C:H films limit their usefulness. They have high compressive stress that limits the maximum film thickness. Reduction of stress or generation of tensile stress is required for applications such as x-ray lithography masks (*76*) and corrosion coatings. They absorb too much visible light for many optical applications, and better thermal stability is required for some tribological applications.

Methods of Preparation of Diamondlike Hydrocarbons

The diamondlike hydrocarbons are formed when hydrocarbon ions hit a substrate with impact energies in the range from fifty to several hundred electron volts. The properties of the film are independent to the type of hydrocarbon precursor and depend primarily on the impact energy and the elemental composition of the source gas (*77*).

The simplest and most widely used method for growing the films is the RF self-bias method. This technique, pioneered by Holland (*78*), is a variation of RF sputtering (*79*). A capacitively coupled electrode in an RF plasma develops a negative bias because of the greatly different mobilities of electrons and positive ions. Ions from the discharge region fall through the potential drop across the sheath to the electrode. Because the gas pressures are high, from 1 to 15 Pa, the ions undergo collisions and therefore acquire a distribution of energies with a mean energy lower than the self-bias potential. Film properties can be controlled by adjusting the pressure and the bias.

At the impact energies employed, on the order of 100 eV, molecular ions disintegrate upon hitting the surface (*80*). This disintegration explains the observed insensitivity of the properties of the films to the particular hydrocarbons used in the plasma. Although large compared to bond energies, the impact energies are much lower than those required for ion implantation. Simple range calculations show that a 100-eV carbon ion will be stopped within 5 to 10 Å of the surface of a carbon target (*81*). Computer simulations have (*82*) showed that the distance of the secondary and tertiary collision cascades is only several angstroms. The entire reaction zone is therefore concentrated in a small volume. The power density dissipated within this surface layer can be high, on the order of 10^6 W cm^{-3}.

The incident ions ($C_mH_n{}^+$) will undergo rapid neutralization and fragmentation. Rössler proposed that the dominant reactions were insertion of the resulting hot neutral carbon atoms into C–H bonds to form acetylenic and olefinic structures

$$C + R\text{–}CH_3 \rightarrow R\text{–}CH{=}CH_2 \qquad (5)$$

The energetic mobile surface layer will be quenched by the underlying cold substrate. Angus and Jansen (*83*) proposed that when the solid film condenses, the composition and average nearest neighbor coordination number adjust so that stabilization by bonding and destabilization by strain energy are balanced. This balance is achieved by the incorporation of hydrogen and trigonally (sp^2) bonded carbon in the carbon skeletal network.

Structure of Diamondlike Hydrocarbons (a–C:H)

A coherent picture of the structure of diamondlike hydrocarbons is emerging (*81, 84, 85*). We describe a–C:H using the constraint-counting method first introduced by Phillips (*86*). According to Phillips, a random covalent network is mechanically constrained when the number of constraints is just equal to the number of mechanical degrees of freedom. The number of constraints per atom can be calculated from the coordination number, that is, the number of directed covalent bonds to nearest neighbors. Increasing the number of bonds contributes to stabilization by virtue of the bond energy. However, increasing the number of directed bonds in a random network leads to increased strain energy because of bond stretching and bond angle distortion. The average coordination number that just uses up the degrees of freedom is the optimal coordination number that balances these two effects.

Angus and Jansen (*83*) have shown that this analysis leads to the following expression for the optimal sp^3/sp^2 in a random covalent network composed solely of sp^2 and sp^3 carbon sites (N_{sp^2} and N_{sp^3}) and hydrogen:

$$\frac{N_{sp^3}}{N_{sp^2}} = \frac{6X_H - 1}{8 - 13X_H} \qquad (6)$$

where X_H is the atom fraction of hydrogen (Fig. 7). Equation 6 indicates that optimally coordinated carbon networks cannot exist at hydrogen atom fractions less than 1/6 or greater than 8/13. If significant amounts of doubly coordinated atoms are present, the lower limit of hydrogen concentration is reduced.

The vertical dashed lines in Fig. 1 are placed at the composition limits predicted by Eq. 6. The agreement between theory and experiment is remarkable and, perhaps, somewhat fortuitous. In Fig. 6 the theoretical sp^3/sp^2 predicted by Eq. 6 and the available experimental data are plotted. The agreement is again good, especially at the high hydrogen concentrations. The rapid increase of sp^3/sp^2 at the critical concentration of $X_H = 8/13$ is clearly evident.

The constraint-counting arguments do not predict how the hydrogen is distributed over the carbon sites. In a nuclear magnetic resonance (NMR) study of a–C:H, Grill *et al.* (*87*) found no evidence of quaternary carbon (carbon bonded to four other carbon atoms). Also, little is present at the other extreme, that is, as $–CH_3$ groups (*88*). The dominant sp^3 sites in that case are either

–C–H or H–C–H

At low hydrogen concentrations, the average coordination number is greater than the optimal value predicted by theory (*83*). The compressive stress caused by this excess of bonding constraints can be relieved partially by the appearance of medium or long range order. The constraint-counting theory does not predict what type of order will develop. In a–C:H, small clusters of sp^2 sites are the most common form of medium range order (*84*). Ramsteiner and Wagner (*89*) have recently obtained direct evidence for these π-bonded clusters with resonant Raman spectroscopy. However, when the RF self-bias method is used with hydrocarbon gases diluted with hydrogen, small diamond crystallites are produced (*90*). This interesting result provides an experimental connection between the preparative methods of a–C:H and crystalline diamond.

Properties of Diamondlike Hydrocarbons (a–C:H)

Diamondlike hydrocarbons have microhardness values ranging between 3000 and 5000 kg mm^{-2}, compared to 2000 to 3500 kg mm^{-2} for silicon carbide. The hardness and wear resistance of a–C:H drops off markedly as the hydrogen content increases (*91*). The films become softer as the proportion of sp^3 sites increases, that is, as the local bonding environment becomes more diamondlike. This behavior may occur because hydrogen, which is monovalent, can serve only as a terminating atom on the carbon skeletal network. However, the average coordination number of carbon to other carbon atoms changes only slightly as the hydrogen content increases, and remains close to the optimal value of 2.4 predicted by theory (*83*). The large decrease in hardness and wear resistance is most likely caused by the development of regions of soft, "polymeric" material as the critical concentration of $X_H = 8/13$ is approached. When these soft or "floppy" regions have percolated through the entire structure, the hardness will decrease greatly and the films will be unable to support large internal compressive stresses (*83, 92*).

The optical gap, which ranges from approximately 0.5 to 2.5 eV, is much less than one would expect for a σ-bonded system. The gap appears to be controlled by π-π* transitions in the π-bonded clusters (*84*). As these clusters grow in size and become more like graphite, the gap decreases. Films that are 1000 Å thick and contain 20 to 30 atomic percent hydrogen appear yellowish brown in transmission. As the hydrogen content increases, the optical gap increases to 2.5 eV and beyond, and the films appear transparent in the visible. These films are, however, polymerlike and soft.

Electrical conductivities of a–C:H range from 10^{-10} to 10^{-16} Ω^{-1} cm^{-1}, consistent with a structure in which the π-bonded clusters are isolated. If the number of sp^2 sites is increased, for example, by annealing the films at 400°C, the conductivity increases dramatically. As the proportion of π-bonded carbon increases, the probability for orbital overlap and enhanced conductivity through extended states increases (*93*). For films doped with B, the logarithm of the conductivity is proportional to $T^{-1/4}$, which indicates that conduction occurs by hopping (*94*).

The permeability of a–C:H is evidently much lower than that of conventional hydrocarbon polymers. For example, the films are inert to organic solvents and inorganic acids, including HF. In addition, argon can remain trapped within 1000 Å diamondlike hydrocarbon films for periods of several years (*83*). Wild and Koidl (*95*) have recently shown that a–C:H is impermeable to hydrocarbon molecules but permeable to H_2.

Diamondlike Carbons (a–C) and Other Phases

Hydrogen-free diamondlike carbon films with a majority of sp^3 carbon sites can also be formed (*96, 97*). These phases appear at atom densities ranging from approximately 0.17 to 0.28 gram-atom per cubic centimeter on Fig. 1.

The key to understanding the structure and properties of the diamondlike carbons (a–C), as in the case with a–C:H, is the ratio of sp^3 to sp^2 sites. Because hydrogen is absent, it cannot be responsible for stabilization of the sp^3 sites. Stress relief in hydrogen-free films with high sp^3/sp^2 is likely achieved by the development of medium-range or long-range order, for example, by clustering or the formation of crystallinity. Study of the structure of these films is complicated because the lack of hydrogen prevents the determination of sp^3/sp^2 site ratio by NMR.

Diamondlike carbon films have been prepared by magnetron sputtering (*97*). These films contain little hydrogen, but are apparently not microcrystalline diamond. By measuring the imaginary part of the dielectric function, $\epsilon(\omega)$, Savvides separated the σ- and π-electron contributions to the optical absorption (*97*). He showed that sp^3/sp^2 decreased from 3 to 1 as the sputtering power density increased. Rossnagel *et al.* (*98*) obtained similar results with magnetron-sputtered carbon. The film properties varied strongly with the deposition conditions, and the more diamondlike properties (high band gap and resistivity) were obtained when less energy was imparted to the growing film by the plasma.

Materials that are loosely called diamondlike carbon may include several different structures ranging from microcrystalline diamond to disordered, amorphous phases. Formation of finely microcrystalline diamond has been reported by Spencer *et al.* (*34*), Kitabatake and Wasa (*51*), and others (*99*).

The ion impact energy plays a critical role in the structure of the deposit. The evidence suggests that microcrystalline diamond cannot form if the impact energy is greater than approximately 100 eV. This value is consistent with the published value for the displacement energy of carbon atoms in diamond of 80 eV (*100*).

Because of the almost infinite bonding possibilities offered by the sp^3 and sp^2 sites, an enormous variety of three-dimensional carbon networks can be imagined. Mertz *et al.* (*101*) have described several continuous networks composed solely of tetrahedrally and trigonally bonded carbon that have not yet been identified experimentally. Some of these phases may be present in the diamondlike carbons. Finally, a superdense carbon phase has been described by Matyusenko *et al.* (*3*). This phase has a calculated density of 4.1 g cm^{-3}, which exceeds the density of crystalline diamond by 15%.

The Future

The commercial production of abrasive grit and diamond-coated tools by low-pressure processes can be expected shortly. Protective coatings and diffusion barriers made of diamondlike phases are being developed for commercial applications now. In the future, an era of diamond-based electronics and optics may be feasible. This application will require much better control of nucleation centers and defects than is possible with current processes. Chemical-vapor deposition processes can more easily be scaled up to produce large crystals than the high-pressure methods. Better understanding and control of the molecular processes involved in diamond nucleation and growth may lead to the production of large-area epitaxy and large single-crystal diamonds. Comparison with silicon vapor-phase epitaxy indicates that linear growth rates of tens of micrometers per hour over areas of many square centimeters might be possible; large crystals could be grown economically at these rates. The development of diamond-growing processes at or near room temperature, perhaps with low-energy ion beams or some of the sophisticated synthetic methods from organic chemistry, is also a long-range possibility.

REFERENCES AND NOTES

1. F. P. Bundy, H. T. Hall, H. M. Strong, R. H. Wentorf, *Nature* **176**, 51 (1955).
2. J. C. Angus, *Thin Solid Films* **142**, 145 (1986).
3. N. N. Matyusenko and V. E. Strel'nitskii, *J. Exp. Theor. Phys. Lett.* **30**, 199 (1979); A. S. Bakai and V. E. Strel'nitskii, *An. Tekh. Fix.* **51**, 2414 (1981).
4. J. E. Field, *Properties of Diamond* (Academic Press, London, 1979), pp. 647–648.
5. D. K. Ferry, *Phys. Rev. B* **12**, 2361 (1975); L. Reggiani *et al.*, *Solid State Commun.* **30**, 333 (1979).
6. S. M. Sze, *Physics of Semiconductor Devices* (Wiley-Interscience, New York, ed. 2, 1981), p. 849.
7. G. Graff, *High Technol.*, p. 44 (April 1987).
8. M. W. Geis *et al.*, *IEEE Elec. Dev. Lett.* **8**, 341 (1987).
9. M. N. Yoder, *Applications of Diamond Technology*, Proceedings of the Second Annual Technology Initiative Seminar, Durham, NC, 7 to 8 July 1987 (Office of Naval Research, Washington, DC, 1987).
10. N. N. Efremow *et al.*, *J. Vac. Sci. Technol.* **B3**, 416 (1985).
11. J. Glinski, X. J. Gu, R. F. Code, H. M. Van Driel, *Appl. Phys. Lett.* **45**, 260 (1984); P. S. Panchii and H. M. Van Driel, *IEEE J. Quant. Elec.* **QE-22**, 101 (1986).
12. M. Rothschild, C. Arnone, D. J. Erlich, *J. Vac. Sci. Technol.* **B4**, 310 (1986); S. Prawer, R. Kalish, M. Adel, *Appl. Phys. Lett.* **48**, 1585 (1986).
13. H. Nakazawa, Y. Kanazawa, M. Kamo, K. Osumi, *Thin Solid Films* **151**, 199 (1987).
14. P. W. Bridgman, *Sci. Am.* **193**, 42 (November 1955).
15. R. C. DeVries, *Annu. Rev. Mater. Sci.* **17**, 161 (1987).
16. P. H. Mohr, personal communication. Mohr was a colleague of W. Eversole during the time of the research on low-pressure diamond growth at the Linde Air Products Company. The experiments are described in A. D. Kiffer, *Synthesis of Diamond from Carbon Monoxide*, report from the Tonawanda Laboratories, Linde Air Products Co., Tonawanda, NY, 6 June 1956; this work appeared as W. G. Eversole, U.S. Patents 3030187 and 3030188 (1962).
17. K. Nassau and J. Nassau, *Lapidary J.*, p. 76 (April 1978); *ibid.*, p. 490 (May 1978).
18. H. Liander and E. Lundblad, *Ark. Kemi* **16**, 139 (1960).
19. B. V. Deryagin and D. V. Fedoseev, *Russ. Chem. Rev.* **39**, 783 (1970); B. V. Deryagin *et al.*, *J. Cryst. Growth* **2**, 380 (1968); B. V. Deryagin and D. V. Fedoseev, *Russ. Chem. Rev.* **39**, 783 (1970); D. V. Fedoseev, B. V. Deryagin, V. P. Varnin, G. K. Sokolina, *Dokl. Akad. Nauk SSSR* **247**, 1201 (1979).
20. B. V. Deryagin and D. V. Fedoseev, *Growth of Diamond and Graphite from the Gas Phase* (Nauka, Moscow, 1977); D. V. Fedoseev, B. V. Deryagin, I. G. Varshavskaya, A. S. Semenova-Tan Shanskaya, *Crystallization of Diamond* (Nauka, Moscow, 1984).
21. A. R. Badzian and R. C. DeVries, *Mater. Res. Bull.* **23**, 385 (1988).
22. J. C. Angus, H. A. Will, W. S. Stanko, *J. Appl. Phys.* **39**, 2915 (1968); D. J. Poferl, N. C. Gardner, J. C. Angus, *ibid.* **44**, 1418 (1973).
23. J. J. Lander and J. Morrison, *Surf. Sci.* **2**, 553 (1964); *J. Chem. Phys.* **34**, 1403 (1963).
24. H. J. Hibshman, U.S. Patent 3371996 (1968); E. C. Vickery, U.S. Patent 3714334 (1970).
25. S. P. Chauhan, J. C. Angus, N. C. Gardner, *J. Appl. Phys.* **47**, 4746 (1976); *J. Vac. Sci. Technol.* **11**, 423 (1974); J. Forgac, thesis, Case Western Reserve University (1978).
26. D. V. Fedoseev, S. P. Vnukov, B. V. Deryagin, *Zh. Fiz. Khim.* **51**, 26 (1977).
27. J. C. Angus *et al.*, *Sint. Almazy* **3**, 38 (1971).
28. B. V. Deryagin and D. V. Fedoseev, *Proceedings of International Conference on Applications of Synthetic Diamonds in Industry*, Kiev, 14 to 18 September 1971 (Naukova Dumka, Kiev, 1971).
29. M. Kitabatake, personal communication.
30. S. Matsumoto, Y. Sato, M. Kamo, N. Setaka, *Jpn. J. Appl. Phys.* **21**, 183, part 2 (1982); S. Matsumoto, Y. Sato, M. Tsutsumi, N. Setaka, *J. Mater. Sci.* **17**, 3106 (1982); M. Kamo, Y. Sato, S. Matsumoto, S. Setaka, *J. Cryst. Growth* **62**, 642 (1983); Y. Matsui, S. Matsumoto, N. Setaka, *J. Mater. Sci. Lett.* **2**, 532 (1983); S. Matsumoto, *ibid.* **4**, 600 (1985); S. Matsumoto, M. Hino, T. Kobayashi, *App. Phys. Lett.* **51**, 737 (1987); S. Matsumoto *et al.*, paper S7-03, 2458, Eighth International Symposium on Plasma Chemistry (ISPC-8), Tokyo (1987).
31. V. P. Varnin *et al.*, *Kristallografiya* **22**, 893 (1977).
32. S. Aisenberg and R. Chabot, *J. Appl. Phys.* **42**, 2953 (1971).
33. C. Weissmantel, *J. Vac. Sci. Technol.* **18**, 179 (1981); Proceedings of the International Ion Engineering Congress—Ion Source and Ion Assisted Technology (ISIAT-83) and Ion Plating and Technologies (IPAT-83), Kyoto, Japan, 1258 (1983); C. Weissmantel, G. Hecht, H. J. Hinneberg, *J. Vac. Sci. Technol.* **17**, 812

(1980); C. Weissmantel *et al.*, *Thin Solid Films* **96**, 32 (1982); C. Weissmantel, in *Thin Films from Free Atoms and Particles*, K. J. Klabunde, Ed. (Academic Press, New York, 1985), p. 153.

34. E. G. Spencer, P. H. Schmidt, D. H. Joy, F. J. Sansalone, *Appl. Phys. Lett.* **29**, 118 (1976).
35. J. H. Freeman, W. Temple, G. A. Gard, *Nature* **275**, 634 (1978); *Vacuum* **34**, 305 (1984).
36. A. R. Patel and K. A. Cherian, *J. Cryst. Growth* **46**, 706 (1979); *Indian J. Pure Appl. Phys.* **119**, 803 (1981).
37. T. Kawato and K. Kondo, *Jpn. J. Appl. Phys.* **26**, 1429 (1987); Y. Hirose and Y. Terasawa, *ibid.* **25**, 1519 (1986).
38. S. Veprek, *J. Cryst. Growth* **17**, 1010 (1972).
39. T. Anthony, Symposium N, fall meeting, Materials Research Society Meeting, Boston, 30 November to 5 December 1985.
40. B. Singh, Y. Arie, A. W. Levine, O. R. Mesker, *Appl. Phys. Lett.* **52**, 451 (1988).
41. K. Suzuki, A. Sawabe, H. Yasuda, T. Inuzuka, *ibid.* **50**, 728 (1987).
42. C. I. H. Ashby, *ibid.* **43**, 609 (1983); *Vac. Sci. Technol.* **2**, 639 (1984).
43. A. Sawabe and T. Inuzuka, *Appl. Phys. Lett.* **46**, 146 (1985).
44. N. Setaka, Proceedings of the Electrochemical Society Meeting, Honolulu, Hawaii, October 1987, p. 1156.
45. M. Kamo *et al.*, Proceeding, Eighth International Symposium on Plasma Chemistry, Tokyo (1987), p. 2481; N. Fujimori, T. Imai, A. Doi, *Vacuum* **36**, 99 (1986); O. Matsumoto, H. Toshima, Y. Kanzaki, *Thin Solid Films* **128**, 341 (1985); O. Matsumoto and T. Katagiri, *ibid.* **146**, 283 (1986).
46. N. Setaka, Symposium N, Materials Research Society Meeting, Boston, 30 November to 5 December 1987; G. Lucovsky, P. V. Tsu, R. J. Markunas, *Mater. Res. Soc. Symp. Proc.* **68**, 323 (1986); S. Matsumoto, M. Hino, T. Kobayashi, *Appl. Phys. Lett.* **51**, 737 (1987).
47. H. Kawarada, K. Sheng Mar, A. Hraki, *Jpn. J. Appl. Phys.* **26**, L1032 (1987); ———, J. Musil, *Vacuum* **36**, 161 (1986).
48. M. Peters *et al.*, paper presented at Society of Photo-Optical Instrumentation Engineers (SPIE), Los Angeles meeting, January 1988.
49. K. Kurihara, K. Sasaki, M. Kawaradi, N. Koshino, *Appl. Phys. Lett.* **52**, 437 (1988).
50. K. Kitahama, K. Hirata, H. Nakamatsu, S. Kawai, *ibid.* **49**, 634 (1986); H. Okabe, R. J. Cody, J. E. Allen, *Chem. Phys.* **92**, 67 (1985); M. P. Irion, K. L. Kompa, *Appl. Phys.* **B27**, 1983 (1982).
51. M. Kitabatake and K. Wasa, *J. Appl. Phys.* **58**, 1693 (1985).
52. A. Sawabe and T. Inuzuka, *Thin Solid Films* **137**, 89 (1986).
53. B. V. Spitsyn, L. L. Bouilov, B. V. Deryagin, *J. Cryst. Growth* **52**, 219 (1981).
54. M. Tsuda, N. Nakajima, S. Oikawa, *J. Am. Chem. Soc.* **108**, 5780 (1986); M. Tsuda, N. Nakajima, S. Oikawa, *Jpn. J. Appl. Phys.* **26**, 1527 (1987).
55. M. Frenklach and K. E. Spear, *J. Mater. Res.* **3**, 133 (1988).
56. R. T. Morrison and R. N. Boyd, *Organic Chemistry* (Allyn and Bacon, Boston, ed. 3, 1976); T. D. Moustakes, Symposium N, Materials Research Society Meeting, Boston, 30 November to 5 December 1987.
57. W. D. Partlow and K. E. Kline, *Mater. Res. Soc. Symp.* **68**, 309 (1986).
58. Y. Sato, M. Kamo, N. Setaka, Proceeding, Eighth International Symposium Plasma Chemistry, Tokyo (1987), p. 2446.
59. M. Sokolowski, *J. Cryst. Growth* **54**, 519 (1981).
60. K. Mitsuda, Y. Kojima, T. Yoshida, K. Akashi, *J. Mater. Sci.* **22**, 1557 (1987).
61. S. Veprek, *Current Topics in Materials Science* (Academic Press, New York, 1984), vol. 4.
62. B. M. Penetrante and E. E. Kinhardt, *J. Appl. Phys.* **59**, 3383 (1986).
63. S. Veprek and W. Peier, *Chem. Phys.* **2**, 478 (1973).
64. K. Nishimura, Symposium N, Materials Research Society Meeting, Boston, 30 November to 5 December 1987.
65. J. W. Faust and H. F. John, *J. Phys. Chem. Solids* **23**, 1119 (1962).
66. F. C. Frank, K. E. Puttick, E. M. Wilks, *Philos. Mag.* **3**, 1261 (1958); J. C. Angus and T. J. Dyble, *Surf. Sci.* **50**, 157 (1975); B. B. Pate, *ibid.* **165**, 83 (1986).
67. J. C. Angus, Proceedings, Defense Advanced Research Projects Agency Workshop on Diamondlike Carbons, BDM Corp., B. Bendow, Ed., Albuquerque, NM, 19 to 20 April 1982.
68. N. Fujimori, Symposium N, Materials Research Society Meeting, Boston, 30 November to 5 December 1987.
69. H. Kawarada *et al.*, *Jpn. J. Appl. Phys.* **26**, L1903 (1987).
70. C. P. Chang, D. L. Flamm, D. E. Ibbotson, J. A. Mucha, *J. Appl. Phys.* **63**, 1744 (1988).
71. T. Anthony, personal communication; S. Mitura, *J. Cryst. Growth* **80**, 417 (1987); B. Deryagin, Symposium N, Materials Research Society Meeting, Boston, 30 November to 5 December 1987.
72. S. Matsumoto and Y. Matsui, *J. Mater. Sci.* **18**, 1785 (1983).
73. H. Schmellenmeier, *Z. Phys. Chem.* **205**, 349 (1955).
74. P. Koidl, A. Bubenzer, B. Dischler, Symposium on Optical Surface Technology, *Proc. Soc. Photo-Opt. Instrum. Eng.* **381**, 186 (1983).
75. M. Kakuchi, M. Hikita, T. Tamamura, *Appl. Phys. Lett.* **48**, 835 (1986).
76. K. H. Muller, P. Tischer, W. Windbracke, *J. Vac. Sci. Technol.* **B4**, 230 (1986); A. W. Yanof, D. J. Resnick, C. A. Jankowski, W. A. Johnson, *Proc. Soc. Photo-Opt. Instrum. Eng.* **632**, 118 (1986).
77. J. Wagner, Ch. Wild, F. Pohl, P. Koidl, *Appl. Phys. Lett.* **48**, 106 (1986); A. Bubenzer, B. Dischler, G. Brandt, P. Koidl, *J. Appl. Phys.* **54**, 4590 (1983); K. Enke, *Appl. Opt.* **24**, 508 (1985).
78. L. Holland, *J. Vac. Sci. Technol.* **14**, 5 (1977); *Thin Solid Films* **58**, 107 (1979).
79. Y. Catherine and P. Couderc, *Thin Solid Films* **144**, 265 (1986); C. B. Zarowin, *J. Appl. Phys.* **57**, 979 (1985).
80. G. S. Selwyn and E. Kay, *Plasma Chem. Plasma Process.* **5**, 1983 (1985).
81. J. C. Angus, P. Koidl, S. Domitz, in *Plasma Deposition of Thin Films*, J. Mort and F. Jansen, Eds. (CRC Press, Boca Raton, FL, 1986), chap. 4.
82. K. Rössler and G. Eich, Proceedings of the European Materials Research Society (E-MRS) Strasbourg Symposium C, 2 to 5 June 1987.
83. J. C. Angus and F. Jansen, *J. Vac. Sci. Technol.* **A6**, 1778 (May/June 1988).
84. J. Robertson and E. P. O'Reilly, *Phys. Rev. B* **35**, 2946 (1987); J. Robertson, *Adv. Phys.* **35**, 317 (1986); J. L. Bredas and G. B. Street, *J. Phys. C* **18**, L651 (1985).
85. H. Tsai and D. B. Bogy, *J. Vac. Sci. Technol.* **A5**, 3287 (1987).
86. J. C. Phillips, *Phys. Rev. Lett.* **42**, 153 (1979).
87. A. Grill *et al.*, *J. Appl. Phys.* **61**, 2874 (1987).
88. B. Dischler, A. Bubenzer, P. Koidl, *Solid State Commun.* **48**, 105 (1983).
89. M. Ramsteiner and J. Wagner, *Appl. Phys. Lett.* **51**, 1335 (1987).
90. K. Kobayashi, N. Mutsukura, Y. Machi, *J. Appl. Phys.* **59**, 910 (1986).
91. F. Jansen, M. Machonkin, S. Kaplan, S. Hark, *J. Vac. Sci. Technol.* **A3**, 605 (1985).
92. M. F. Thorpe, *J. Non-Cryst. Solids* **57**, 355 (1983).
93. R. J. Gambino and J. A. Thomson, *Solid State Commun.* **34**, 15 (1980); E. T. Prince and M. M. Romach, *J. Vac. Sci. Technol.* **A3**, 694 (1985).
94. B. Meyerson and F. W. Smith, *Solid State Commun.* **34**, 531 (1980); *ibid.* **41**, 23 (1982).
95. Ch. Wild and P. Koidl, *Appl. Phys. Lett.* **51**, 1506 (1987).
96. V. E. Strel'nitskii, V. G. Padalka, S. I. Vakula, *Sov. Phys. Tech. Phys.* **23**, 222 (1978); T. Miyazawa, S. Misawa, S. Yoshida, S. Gonda, *J. Appl. Phys.* **55**, 188 (1985); J. W. Rabelais and S. Kasi, *Science* **239**, 623 (1988).
97. N. Savvides, *J. Appl. Phys.* **58**, 518 (1985); *ibid.* **59**, 4133 (1986); N. Savvides and B. Window, *J. Vac. Sci. Technol.* **A3**, 2386 (1985).
98. S. M. Rossnagel, M. A. Russak, J. J. Cuomo, *J. Vac. Sci. Technol.* **A5**, 2150 (1987).
99. T. Mori and Y. Namba, *ibid.* **A1**, 23 (1983); K. Fujii, N. Shohata, M. Mikami, M. Yonezawa, *Appl. Phys. Lett.* **47**, 370 (1985); H. Kojima, H. Kako, M. Terada, H. Sugai, T. Okuda, *Jpn. J. Appl. Phys.* **24**, 1432 (1985); Z. Has and S. Mirta, *Thin Solid Films* **128**, 353 (1985).
100. E. A. Burgermeister, C. A. J. Ammerlaan, G. Davies, *J. Phys. C* **13**, L691 (1980).
101. K. M. Merz, R. Hoffman, A. T. Balaban, *J. Am. Chem. Soc.* **109**, 6742 (1987).
102. J. Fink *et al.*, *Phys. Rev. B* **30**, 4713 (1984).
103. K. Fujii, S. H. Yokata, S. Shohata, *Mater. Res. Soc. Symp. Proc.* **75**, 765 (1987).
104. S. Kaplan, F. Jansen, M. Machonkin, *Appl. Phys. Lett.* **47**, 750 (1985).
105. A. R. Nyaeish, R. E. Kirby, F. K. King, E. L. Garwin, *J. Vac. Sci. Technol.* **A3**, 610 (1985).
106. C. Weissmantel, *ibid.* **A3**, 2384 (1985).
107. One of the authors (J.C.A.) acknowledges the contributions of several generations of graduate students: H. A. Will, W. S. Stanko, T. J. Dyble, D. J. Poferl, J. M. Forgac, S. P. Chauhan, C. Smith, J. Bishop, and P. Shiller.